Electric field sampling of modelocked pulses from a quantum cascade laser

Joshua R. Freeman,[1*] Jean Maysonnave,[1] Harvey E. Beere,[2] David A. Ritchie,[2] Jérôme Tignon,[1] and Sukhdeep S. Dhillon[1]

[1]*Laboratoire Pierre Aigrain, Ecole Normale Supérieure, CNRS (UMR 8551), Université P. et M. Curie, Université D. Diderot, 75231 Paris Cedex 05, France*
[2]*Semiconductor Physics, Cavendish Laboratory, University of Cambridge, JJ Thomson Avenue, Cambridge, CB3 0HE, UK.*
[*]*freeman@lpa.ens.fr*

Abstract: We measure the electric field of a train of modelocked pulses from a quantum cascade laser in the time-domain by electro-optic sampling. The method relies on synchronizing the modelocked pulses to a reference laser and is applied to 15-ps pulses generated by a 2-THz quantum cascade laser. The pulses from the actively modelocked laser are completely characterized in field and in time with a sub-ps resolution, allowing us to determine the amplitude and phase of each cavity mode. The technique can also give access to the carrier-envelope phase of each pulse.

OCIS codes: (140.4050) Mode-locked lasers; (140.5965) Semiconductor lasers, quantum cascade; (320.7100) Ultrafast measurements.

References and links

1. A. E. Siegman, *Lasers* (University Science books, 1989).
2. R. Trebino, *Frequency-Resolved Optical Gating: The Measurement of Ultrashort Laser Pulses* (Springer, 2002).
3. C. Iaconis and I. Walmsley, "Spectral phase interferometry for direct electric-field reconstruction of ultrashort optical pulses," Opt. Lett. **23**, 792–794 (1998).
4. I. A. Walmsley and C. Dorrer, "Characterization of ultrashort electromagnetic pulses," Adv. Opt. Photon. **1**, 308–437 (2009).
5. Y.-S. Lee, *Principles of Terahertz Science and Technology* (Springer, New York, 2009).
6. R. Paiella, *Intersubband Transitions in Quantum Structures* (McGraw-Hill, 2006).
7. J. Devenson, R. Teissier, O. Cathabard, and A. N. Baranov, "InAs/AlSb quantum cascade lasers emitting below 3μm," Appl. Phys. Lett. **90**, 111118 (2007).
8. G. Scalari, C. Walther, M. Fischer, R. Terazzi, H. Beere, D. Ritchie, and J. Faist, "THz and sub-THz quantum cascade lasers," Laser and Photonics Review **3**, 45–66 (2009).
9. S. Barbieri, M. Ravaro, P. Gellie, G. Santarelli, C. Manquest, C. Sirtori, S. P. Khanna, E. H. Linfield, and A. G. Davies, "Coherent sampling of active mode-locked terahertz quantum cascade lasers and frequency synthesis," Nat. Photon. **5**, 306–313 (2011).
10. J. R. Freeman, J. Maysonnave, N. Jukam, P. Cavalie, K. Maussang, H. E. Beere, D. A. Ritchie, J. Mangeney, S. S. Dhillon, and J. Tignon, "Direct intensity sampling of a modelocked terahertz quantum cascade laser," Appl. Phys. Lett. **101**, 181115 (2012).
11. J. Maysonnave, K. Maussang, J. R. Freeman, N. Jukam, J. Madéo, P. Cavalié, R. Rungsawang, S. Khanna, E. Linfield, A. Davies, H. Beere, D. Ritchie, S. Dhillon, and J. Tignon, "Mode-locking of a terahertz laser by direct phase synchronization," Opt. Express **20**, 20855–20862 (2012).
12. D. Oustinov, N. Jukam, R. Rungsawang, J. Madeo, S. Barbieri, P. Filloux, C. Sirtori, X. Marcadet, J. Tignon, and S. Dhillon, "Phase seeding of a terahertz quantum cascade laser," Nat. Commun. **1**, 69 (2010).
13. J. Maysonnave, N. Jukam, M. S. M. Ibrahim, R. Rungsawang, K. Maussang, J. Madéo, P. Cavalié, P. Dean, S. P. Khanna, D. P. Steenson, E. H. Linfield, A. G. Davies, S. S. Dhillon, and J. Tignon, "Measuring the sampling coherence of a terahertz quantum cascade laser," Opt. Express **20**, 16662–16670 (2012).

#189788 - $15.00 USD Received 30 Apr 2013; revised 14 Jun 2013; accepted 17 Jun 2013; published 28 Jun 2013

14. J. R. Freeman, J. Maysonnave, S. Khanna, E. H. Linfield, A. G. Davies, S. S. Dhillon, and J. Tignon, "Laser-seeding dynamics with few-cycle pulses: Maxwell-bloch finite-difference time-domain simulations of terahertz quantum cascade lasers," Phys. Rev. A **87**, 063817 (2013).
15. C. Y. Wang, L. Kuznetsova, V. M. Gkortsas, L. Diehl, F. X. Kartner, M. A. Belkin, A. Belyanin, X. Li, D. Ham, H. Schneider, P. Grant, C. Y. Song, S. Haffouz, Z. R. Wasilewski, H. Liu, and F. Capasso, "Mode-locked pulses from mid-infrared quantum cascade lasers," Opt. Express **17**, 12929–12943 (2009).
16. J. R. Freeman, O. P. Marshall, H. E. Beere, and D. A. Ritchie, "Improved wall-plug efficiency of a 1.9THz quantum cascade laser by an automated design approach," Appl. Phys. Lett. **93**, 191119 (2008).
17. P. Gellie, S. Barbieri, J.-F. Lampin, P. Filloux, C. Manquest, C. Sirtori, I. Sagnes, S. P. Khanna, E. H. Linfield, A. G. Davies, H. Beere, and D. Ritchie, "Injection-locking of terahertz quantum cascade lasers up to 35ghz using rf amplitude modulation," Opt. Express **18**, 20799–20816 (2010).
18. C. Kubler, R. Huber, S. Tubel, and A. Leitenstorfer, "Ultrabroadband detection of multi-terahertz field transients with gase electro-optic sensors: Approaching the near infrared," Appl. Phys. Lett. **85**, 3360–3362 (2004).
19. A. Hugi, R. Terazzi, Y. Bonetti, A. Wittmann, M. Fischer, M. Beck, J. Faist, and E. Gini, "External cavity quantum cascade laser tunable from 7.6 to 11.4 μm," Appl. Phys. Lett. **95**, 061103 (2009).
20. E. Goulielmakis, M. Schultze, M. Hofstetter, V. S. Yakovlev, J. Gagnon, M. Uiberacker, A. L. Aquila, E. M. Gullikson, D. T. Attwood, R. Kienberger, F. Krausz, and U. Kleineberg, "Single-cycle nonlinear optics," Science **320**, 1614–1617 (2008).

1. Introduction

Modelocked lasers are widely used in both science and industrial applications in areas as diverse as non-linear optics, micromachining, two-photon microscopy, nuclear fusion and more recently optical frequency combs [1]. Since the earliest demonstrations of modelocked pulses considerable work has been done to properly characterize them and many methods have been developed. These can be divided in two groups; spectrographic techniques based on frequency-resolved-optical-gating (FROG) [2] and interferometric techniques based on Spectral Phase Interferometry for Direct Electric Field Reconstruction (SPIDER) [3]. All these methods rely on pulse reconstruction algorithms to determine the electric field of the modelocked pulse, from the measured spectrographic or interferometric data. While these techniques have proved extremely useful for the characterization of ultrafast pulses, care must be taken with the reconstruction; particularly the direction-of-time ambiguity in FROG and calibration of the delay in SPIDER. In addition, neither of these techniques gives access to the carrier-envelope phase. An extensive review of these and related methods can be found in [2, 4].

In this work we demonstrate a technique to directly measure the electric field of a modelocked laser. The technique relies on the availability of a second, reference, laser source which produces pulses sufficiently short to sample the electric field of the modelocked pulses under investigation, as in THz time-domain spectroscopy [5]. The sampling method used in this work is viable because of the very different time-scales involved with the two lasers that we use. A pulse length of 80 fs for the Ti:Sapphire reference pulse provides the 'timing' and is used to sample a modelocked THz pulse (where the period of the electric field is around 500 fs). Because of the need for a reference laser, this technique is not self-referencing like FROG and SPIDER, thus there is a limitation on the wavelengths that maybe detected, dictated by the duration of the reference laser pulse. However it does provide a complete description of the electric field of the pulse, including the carrier-envelope phase. We show below that it would be possible to control this quantity with suitable feedback.

The modelocked laser pulses that we study are generated by a quantum cascade laser. Quantum cascade lasers (QCLs) are unipolar semiconductor lasers with the laser transition between two confined conduction band states within a heterostructure [6]. Because the emission frequency depends only on the heterostructure, the emission frequency can be tailored by design, QCLs currently operate with emission wavelengths from below 3 μm [7] to 250 μm [8]. In this work we use a QCL operating in the THz range, with a wavelength of 155 μm.

Active modelocking in THz QCLs has recently been demonstrated, firstly by Barbieri *et al.*

#189788 - $15.00 USD Received 30 Apr 2013; revised 14 Jun 2013; accepted 17 Jun 2013; published 28 Jun 2013

[9] and more recently by the present authors [10]. In both cases, and in this work, the modelocking was achieved by a modulation of the QCL drive current at the cavity round-trip frequency. The coherent measurement of Barbieri *et al.* relied on an asynchronous sampling technique with active phase stabilization to record both frequency- and time-domain information with a temporal resolution of 2.3 ps, about 6 electric field cycles. Besides the improved resolution, an important difference between the present work and that of [9] is that here the QCL is gain-switched so that each pulse detected is referenced to the switch-on of the laser. In [10], our previous work, the QCL was not seeded and the measurement was not coherent so that frequency information was not collected in the same measurement and no information on the carrier-envelope phase was available. Another demonstration of modelocking with THz QCLs [11] did not use active modulation but relied on a short cavity and phase-seeding by pulse injection to achieve modelocking operation. However, further measurements showed that the pulses were not stable over longer times ($>$1 ns) since no stabilization, either passive or active, was used. Another previous work [12] demonstrated coherent measurements of a THz QCL, but the QCL was not modelocked in that case.

2. Electric field sampling

The experimental arrangement is shown in Fig. 1. The detection of the modelocked THz pulses from the QCL relies on synchronizing the phase of the THz electric field with a reference femtosecond laser. The reference laser we use is a Ti:Sapphire laser operating at around 800 nm producing 80-fs pulses at a repetition rate of 76.47 MHz. The THz electric field is measured by electro-optic sampling, where the change in polarization induced in the reference laser by the instantaneous THz electric field present in the nonlinear crystal (1 mm ZnTe in the present case) [5]. Time-resolved measurements of the THz field is achieved by changing the optical delay between the femtosecond probe pulse and the modelocked pulse train by moving the optical delay line. For a fixed delay, the instantaneous value of THz field is recovered via summation of a large number of sampling events, due to the limited speed of the electronics. Consequently, detection is only possible if successive reference laser pulses sample the same point in the THz field so the sampling events add constructively.

This synchronization is achieved by optical injection seeding of the THz QCL cavity using a broadband THz pulse generated by focusing the 800nm reference pulse onto a biased GaAs photoconductive antenna. The injected broadband THz pulse arrives at the same moment that QCL gain is brought above threshold using a gain-switching nanosecond pulse, also triggered by the reference pulse. This seeding procedure ensures that the QCL emission is initiated by the injected broadband THz pulse rather than the spontaneous emission and is described fully by Oustinov *et al.* [12]. Otherwise put, the field emitted from the QCL is the same each time the QCL is switched-on. The effect the optical seed on the laser operation is thought to be important only for the first $\sim$500-ps of the emission; in ref. [13] it was found that a seed pulse will decrease the build-up time of the emssion, these results we confirmed by simulations, which additionally showed that after this start-up time, the emission closely resembles the 'free-running' emission [14]. From QCL output power measurements we estimate that the gain-switching pulse provides 200mA, so the threshold for the quasi-DC when the pulse applied is 445 mA. The quasi-DC is modulated at 10 kHz and 10% duty-cycle to reduce heating in the sample compared to a true DC current and is also used for the lock-in detection. The photoconductive antenna is biased at 20 kHz and a 20% duty cycle to ensure that the signal from the antenna is not directly detected by the lock-in amplifier.

In addition to synchronizing the THz field, it is necessary to ensure that the round-trip (RT) modulation applied to modelock the QCL is an integer multiple of the reference laser repetition rate. This is required so that for a fixed optical delay the reference probe pulse will always

#189788 - $15.00 USD Received 30 Apr 2013; revised 14 Jun 2013; accepted 17 Jun 2013; published 28 Jun 2013

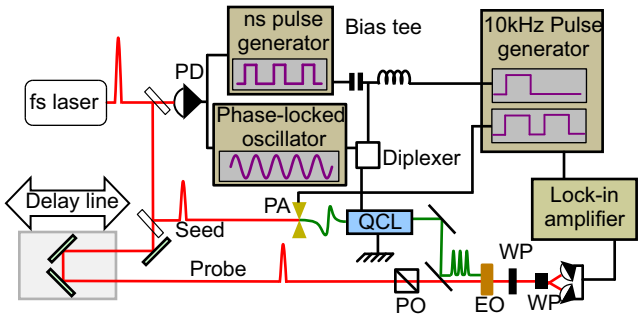

Fig. 1. Experimental arrangement for electric field measurement of modelocked pulses. The nanosecond pulse generator comprises an Agilent 81160A 500-MHz function generator and a broadband (6 GHz bandwidth) high power amplifier. The labels indicate: PA - Photoconductive antenna, PD - fast photodiode, PO- polarizer, EO - electro-optic crystal (1 mm ZnTe), WP - quarter-wave plate, WP - Wollaston prism.

sample the same point in the envelope of the THz field. To achieve this integer link we use a fast photodiode, a tunable Yttrium Iron Garnet (YIG) bandpass filter and an amplifier chain to obtain the 170th harmonic of the reference laser repetition rate (170×76.47 MHz=13.00 GHz), described in [10]. This arrangement is labeled as 'Phase-locked oscillator' in Fig. 1. As shown previously in [15] and [10], to achieve modelocking in QCLs the device must be biased close to threshold and strong RT modulation powers must be used. Furthermore, for a fixed modulation power, pulse width tends to increase as the DC, or quasi-DC, bias point is increased. For this reason the QCL used in this study was biased either just above or below threshold to ensure short pulses. The RT modulation powers that we quote here have been corrected for an estimated 10 dB loss in cables, connections and coupling between the phase-locked oscillator and the QCL. We have verified that all the field emitted by the QCL is detected by evaluating the sampling coherence using the technique described in [13]. We find close to 100% of the QCL field is synchronized to the reference laser.

3. Results

The QCL active region is described in [16] and was processed into a single plasmon waveguide, 3 mm long and 250 μm wide. The QCL was indium soldered onto a copper sub-mount and one end was wire-bonded to a coplanar waveguide with an impedance of 50 Ω, matched to a high-frequency coaxial cable. The QCL was operated at 10 K for all of the measurements shown here.

This active region operates with a center frequency of 1.93 THz and was chosen because of the high slope efficiency, which allows a large gain modulation depth to be achieved. The emission from this active region is not broad, showing only one significant mode above threshold for most of the lasing range, however, this does not prevent modelocking because the strong modulation that is applied generates sidebands in the frequency domain [17].

A comparison between the phase-resolved emission detected from the sample with and without RT modulation applied is shown in Fig. 2, together with the corresponding fast Fourier transform (FFT) for each. We have chosen to study the emission from around 1 ns after the switch-on of the laser because after this time the laser reaches a steady-state; the switch-on time is thought to be limited by the rise time of the gain-switching pulse. The FFT of the 1.5-ns long signal yields the laser mode spectrum with a resolution (0.66 GHz) higher than is available using typical a Fourier-transform-infrared (FTIR) spectrometer (6 GHz). Figure 2 shows

#189788 - $15.00 USD Received 30 Apr 2013; revised 14 Jun 2013; accepted 17 Jun 2013; published 28 Jun 2013

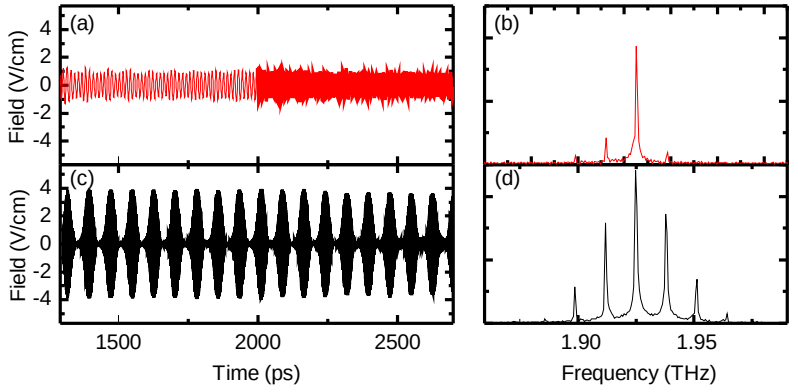

Fig. 2. (a) The electric field measured from the QCL when biased just above threshold and no modulation is applied, (b) the corresponding FFT. The mode spacing of 13.01 GHz for the 3-mm device implies a refractive index of 3.84. (c) The same bias point when a 21-dBm modulation at 13.00 GHz is applied to the cavity and (d) the corresponding FFT. The seed arrives at 0 ps, the same moment the laser is switched on with the gain-switching pulse.

the case when the laser is biased just above threshold with a quasi-DC of 450 mA and a RT modulation of 21 dBm at 13.00 GHz is applied to the cavity in Figs. 2(c) and 2(d). The effect of the modulation is very clear, going from a quasi-CW emission to modelocked pulses when the modulation is applied. The spectra are correspondingly affected; when the RT modulation is applied the spectrum broadens to include 6 modes rather than the 3 present when there is no modulation applied. Besides the benefits of the coherent detection giving both the phase and amplitude of the electric field we also have a higher signal-to-noise ratio than the intensity sampling method previously used in [10].

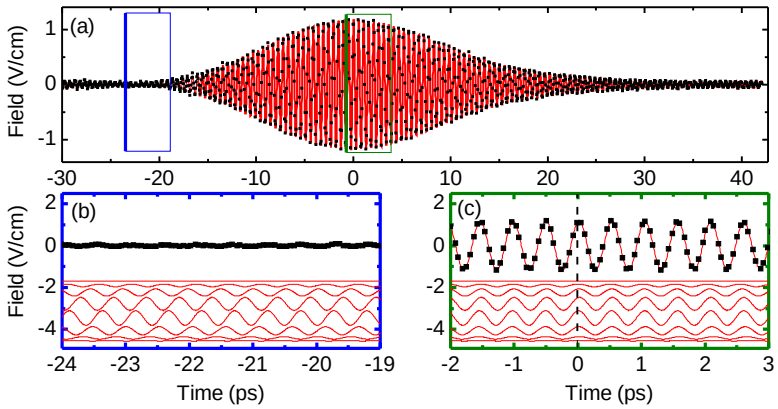

Fig. 3. (a) A pulse centered at 1983 ps (normalized to zero), data in black points, the fit is shown in red. (b) Zoom of the same pulse between -24 and -19 ps together with the component modes (c) Zoom between -2 and 3 ps together with the component modes, shown that the modes add constructively. The dashed line indicates the envelope maximum as t=0 ps.

#189788 - $15.00 USD Received 30 Apr 2013; revised 14 Jun 2013; accepted 17 Jun 2013; published 28 Jun 2013

Now that the longitudinal laser modes present in the emission are known, we can use this information to find the amplitude and phase of each mode using a fitting technique. To do this we take a single pulse, as shown in Fig. 3, and fit the function

$$f(t) = \sum_n a_n \cos(2\pi \nu_n (t - t_p) + \phi_n). \quad (1)$$

Here, ν_n is the frequency of the nth mode, found from the FFT and t_p is the position of the envelope maximum. We normalize the position of the maximum to ensure that a perfectly modelocked pulse corresponds to the case when all phases are equal, which also aids the comparison between pulses. The values of the amplitude, a_n, and the phase, ϕ_n, of the nth mode are found from the fitting. This fitting procedure is summarized in Fig. 3. To reduce the pulse width for this case, we have reduced the quasi-DC to 405 mA so that the laser is below threshold and increased the power of the RT modulation to 23 dBm [10]. Figure 3(a) shows a modelocked pulse that has been fitted with the function above. The sampled data are shown by black marks and the fit is shown as a red continuous line. Two areas have been highlighted, shown in Figs. 3(b) and 3(c), to show the case when the modes sum destructively and constructively, respectively. The lower portion of these figures show the oscillations of each of the modes that add to produce the fit; it can be clearly seen that these add destructively in Fig. 3(b) and constructively in 3(c). The maximum of the envelope, normalized to 0 ps, is also shown with a dashed line in Fig. 3(c). We find that the fit to the data is excellent for all pulses with an average R^2=0.995.

This fitting procedure is carried out for each pulse in the pulse train and summarized in Fig. 4. Figure 4(a), shows the electric field of the sampled pulse train between 800 ps and 2700 ps and comprises 25 pulses. The width of these pulses is 15 ps, corresponding to around 29 optical cycles. The phase of each mode, relative to the most intense mode, is shown in Fig. 4(b) for each pulse. We see that although we fit 8 modes there are only 6 with any significant power, the amplitudes of which are stable in time. The phases of the modes are also relatively stable, the six modes plotted have phases in the range ± 0.3 radians. The four most intense modes have phases in the range ± 0.15 radians, indicating that there is good phase synchronization between the modes. It is also interesting to note that we also have access to the carrier-envelope phase shift for each modelocked pulse, a quantity that becomes important for pulses with few optical cycles and not a quantity that is available through techniques such as FROG or SPIDER. In the present case the relatively long pulses (29 optical cycles) prevents a determination of the pulse envelope position (and hence the carrier envelope phase) with the required accuracy. However, this uncertainty reduces with shorter pulses when this quantity becomes important.

To further aid interpretation and comparison with other methods for characterization of modelocked pulses we have also plotted, in Fig. 4(c), the amplitude and phase information in a more conventional way. For this case we have taken the FFT of each pulse separately and plotted all points on the same axis for both the amplitude (black squares) and phase (orange circles). To ensure a comparison with the phase information retrieved from the fitting procedure we normalized the temporal position of each pulse to zero before taking the FFT to obtain an average gradient for the phase vs. frequency of zero [2]. We have also plotted the average values for the phase of each mode found from the fitting in Fig. 4(b), these clearly shown the same trend, confirming that the two methods (fitting vs. FFT) measure the same qualities. The almost linear dependence of the phase on the frequency indicates that the pulses are very close to being Fourier-transform limited.

4. Effect of modulation frequency

As a further demonstration of the detection technique and the control we are able to exercise over the pulse train we have recorded the pulse trains for different applied modulation frequencies. Frequencies between 12.56 and 13.30 GHz were applied, above and below the 'natural'

#189788 - $15.00 USD Received 30 Apr 2013; revised 14 Jun 2013; accepted 17 Jun 2013; published 28 Jun 2013

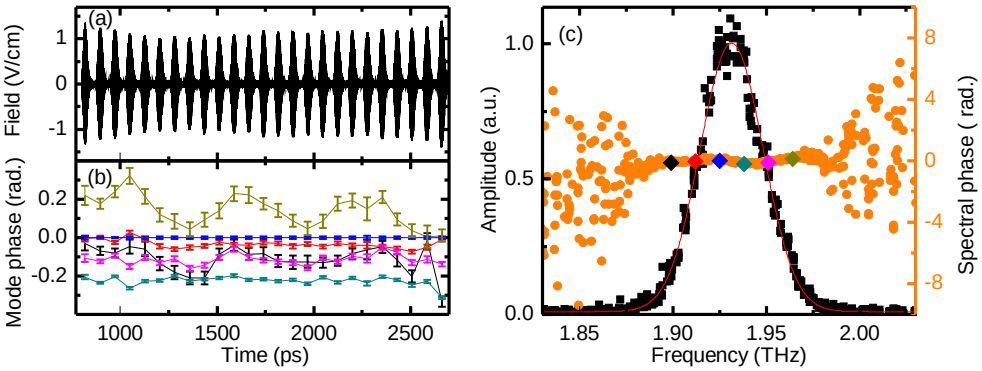

Fig. 4. (a) Electric field measured from the modelocked QCL, showing a train of 25 pulses. The average pulse width (intensity) is 15 ps (equivalent to around 29 electric field cycles). (b) Results from fitting each pulse, the phases of the six most intense modes are show. (c) The amplitude and phase found from taking the FFT of each pulse. The amplitude (black squares) is fitted with a Gaussian curve (red). The phase (pink circles) found from the FFT is plotted together with the average phases found for each mode from the fitting (colored diamonds).

cavity round-trip time of 13.00 GHz. As mentioned above, the applied frequencies are separated by 76.47 MHz owing to the need to apply a RT frequency that is an integer multiple of the reference laser repetition frequency.

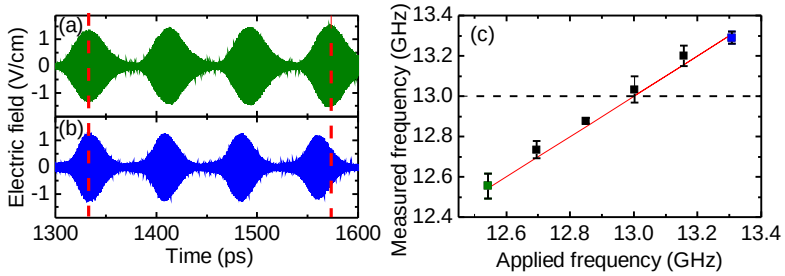

Fig. 5. (a) The modelocked pulse trains for applied RT modulation 12.54 GHz. The dashed lines mark the first and fourth pulses in to aid the comparison. (b) Corresponding data for an applied frequency of 13.30 GHz. Note that the direction of the asymmetry changes if the applied frequency is above or below the resonance. (c) The measured modelocked pulse repetition rate as a function of applied modulation frequency. The solid red line is the case for $\nu_{\text{applied}} = \nu_{\text{measured}}$. The dashed black line indicates the RT frequency when no modulation is applied.

Figures 5(a) and 5(b) show a train of four pulses for an applied modulation of (a) 12.54 GHz and (b) 13.30 GHz. It is immediately clear that changing the applied frequency changes the pulse repetition rate. It is also interesting to note that the direction of the pulse asymmetry changes, depending on whether the applied modulation is above or below the natural cavity round-trip time. This change in asymmetry can be understood in an intuitive way by considering that pulses circulating at a frequency slightly higher than the modulation frequency ($\nu_{\text{applied}} < \nu_{\text{RT}}$) will tend to see more amplification of the trailing edge of the pulse, while pulses with $\nu_{\text{applied}} > \nu_{\text{RT}}$ will tend to see more amplification of the leading edge of the pulse. In Fig. 5(c)

#189788 - $15.00 USD Received 30 Apr 2013; revised 14 Jun 2013; accepted 17 Jun 2013; published 28 Jun 2013

we have plotted the dependence on the measured round-trip frequency (found from the mode spacing in the FFT of each pulse train) on the frequency applied to the QCL cavity. The red line is not a fit, but represents the case of $\nu_{\text{applied}}=\nu_{\text{measured}}$. It is clearly seen that the measured frequency follows the applied frequency to within the error of the measurement. This implies that we are able to control the envelope of the pulse circulating in the cavity independently from the THz carrier frequency. Thus, with appropriate feedback on the frequency and phase of the applied RT frequency, we could control the carrier-envelope phase such that all pulses had the same, user selected, carrier-envelope phase. In practice the control of the applied frequency would be achieved by changing the reference laser repetition rate through tuning the cavity length of that laser in order to maintain the integer relation between the reference laser repetition frequency and the cavity modulation frequency. When the applied frequency lies outside the frequency range above, the amplitude of the pulses decreases significantly and there is larger continuous component to the emission.

By combining a suitable non-linear medium and phase-locking, this sampling method could be extended to measure ultrashort pulses beyond the THz range. The obvious limitation of this method is the requirement for a reference laser that is short enough to sample the oscillating electric field of the laser under investigation. The highest frequency of a signal that can be sampled is given by the Nyquist-Shannon sampling theorem as $\frac{1}{2\Delta t}$, where Δt is the time step between samples. Assuming time steps of 10fs, roughly the current pulse length limit of easily available femtosecond sources, one finds the minimum wavelength that could be sampled is 6 μm. Furthermore, Kubler *et al.* [18] report generation and detection wavelengths as short as 2.5 μm by electro-optic interactions using 10-fs pulses.This limit is well within the range of QCLs operating in the mid-infrared region which operate at room temperature (Hugi *et al.* [19] give several high performance designs operating between 7.6 and 11.4 μm) and can be modelocked with similar techniques to those used here [15].

5. Conclusions

We have demonstrated time-resolved electric field detection of modelocked laser pulses. For each pulse generated we are able to extract the field profile and the amplitude/phase of each mode by fitting the electric field. The technique relies on triggering the laser with a gain-switching pulse, meaning that in contrast to FROG and SPIDER techniques we are able to distinguish between different pulses in the resulting pulse train. This also gives access to the dynamics of modelocking, such as the build-up regime.

In addition we have shown that we have control over the envelope of the emission and therefore, in principle over the carrier-envelope shift. With appropriate feedback this could be controlled from pulse to pulse, allowing frequency metrology to be brought to the THz domain. Indeed, taking this technique to its limit by using attosecond pulses [20], it would be possible to measure electric fields of modelocked lasers in the optical domain.

Acknowledgments

This work was supported by the 'Agence Nationale de la Recherche' (ANR, contract 'HI-TEQ' ANR-09-NANO-017). One author (J.R.F) acknowledges funding from a Marie Curie fellowship (Grant No. 274602).

#189788 - $15.00 USD Received 30 Apr 2013; revised 14 Jun 2013; accepted 17 Jun 2013; published 28 Jun 2013